

Intriguing Aspects of Lanthanide Luminescence

Jean-Claude G. Bünzli^{a,b} and Svetlana V. Eliseeva^{c,d}

Received (in XXX, XXX) Xth XXXXXXXXXX 20XX, Accepted Xth XXXXXXXXXX 20XX

DOI: 10.1039/C2SC2xxx

Electronic Supplementary Information (10 pages)

Executive Summary of Lanthanoid Photophysics

Trivalent lanthanide ions only are considered here. Their photophysics, i.e. absorption and emission spectra, is fairly well understood. Indeed, simple models such as Russel-Saunders scheme for describing spin-orbit coupling, ligand-field theory for understanding the splitting of the electronic levels in compounds, and Judd-Ofelt parameterization for reproducing the intensity of f-f transitions, apply fairly well in view of the weak ligand-field effects (a few hundred of cm^{-1} only). The reader interested in more details is referred to reviews by C. Görller-Walrand and K. Binnemans on rationalization of ligand-field parameterization¹ and spectral intensities of f-f transitions² are very useful and easy to read, with careful and precise definitions as well as very helpful dimensional analysis. More recently, the book edited by G. K. Liu and B. Jacquier³ sheds light on lanthanoid-containing optical materials while Judd-Ofelt theory has been summarized in an elegant way by B. M. Walsh.⁴ Applications of lanthanoid luminescence in biosciences are summarized in a multi author book edited by P. Hänninen and H. Härmä published in 2011⁵ and which contains an introductory description of lanthanoid photophysics intended for a broad readership in science with minimum background in physics and mathematics.⁶

1. *Electronic Configurations*

The ground state electronic configuration of Ln^{III} ions is $[\text{Xe}]4f^n$ ($n = 0-14$). It is well separated in energy from the $[\text{Xe}]4f^{n-1}5d^1$ configuration ($\Delta E > 32\,000\text{ cm}^{-1}$) so that little interaction with the latter configuration is expected. Each 4f electron is associated with one of the seven 4f wavefunctions and may have a spin of $+\frac{1}{2}$ or $-\frac{1}{2}$. Simple combinatorial considerations show that there are numerous ways of associating the n electrons with the seven 4f orbitals, taking spin values into consideration. This leads to large multiplicities of the configurations.

Table 1 summarizes the situation, where a spectroscopic term is defined by the two quantum numbers S and L while a spectroscopic level is additionally characterized by a third quantum number, J . A partial energy level diagram is given on Figure 1. When the ions are introduced into chemical compounds, the $(2J+1)$ degenerate electronic levels split under the influence of ligand-field potential. The numbers of ligand-field sublevels depend on the value of J and are collected in Table 2 versus the site symmetry.

Table 1. Electronic properties of the Ln^{III} ions.

f ⁿ	Multi- plicity	Nr of terms	Nr of levels	Ground level		λ/cm^{-1} ^a	
f ⁰	f ¹⁴	1	1	¹ S ₀	¹ S ₀	0	0
f ¹	f ¹³	14	1	² F _{5/2}	² F _{7/2}	625	-2870
f ²	f ¹²	91	7	³ H ₄	³ H ₆	370	-1314
f ³	f ¹¹	364	17	⁴ I _{9/2}	⁴ I _{15/2}	295	-793
f ⁴	f ¹⁰	1001	47	⁵ I ₄	⁵ I ₈	250	-535
f ⁵	f ⁹	2002	73	⁶ H _{5/2}	⁶ H _{15/2}	231	-386
f ⁶	f ⁸	3003	119	⁷ F ₀	⁷ F ₆	221	-285
f ⁷		3432	119	⁸ S _{7/2}			0

^a Spin-orbit constant; for aqua ions,⁷ except in the cases of Ce^{III} (Ce:LaCl₃) and Yb^{III} (Yb₃Ga₅O₁₂), taken from ref.⁸

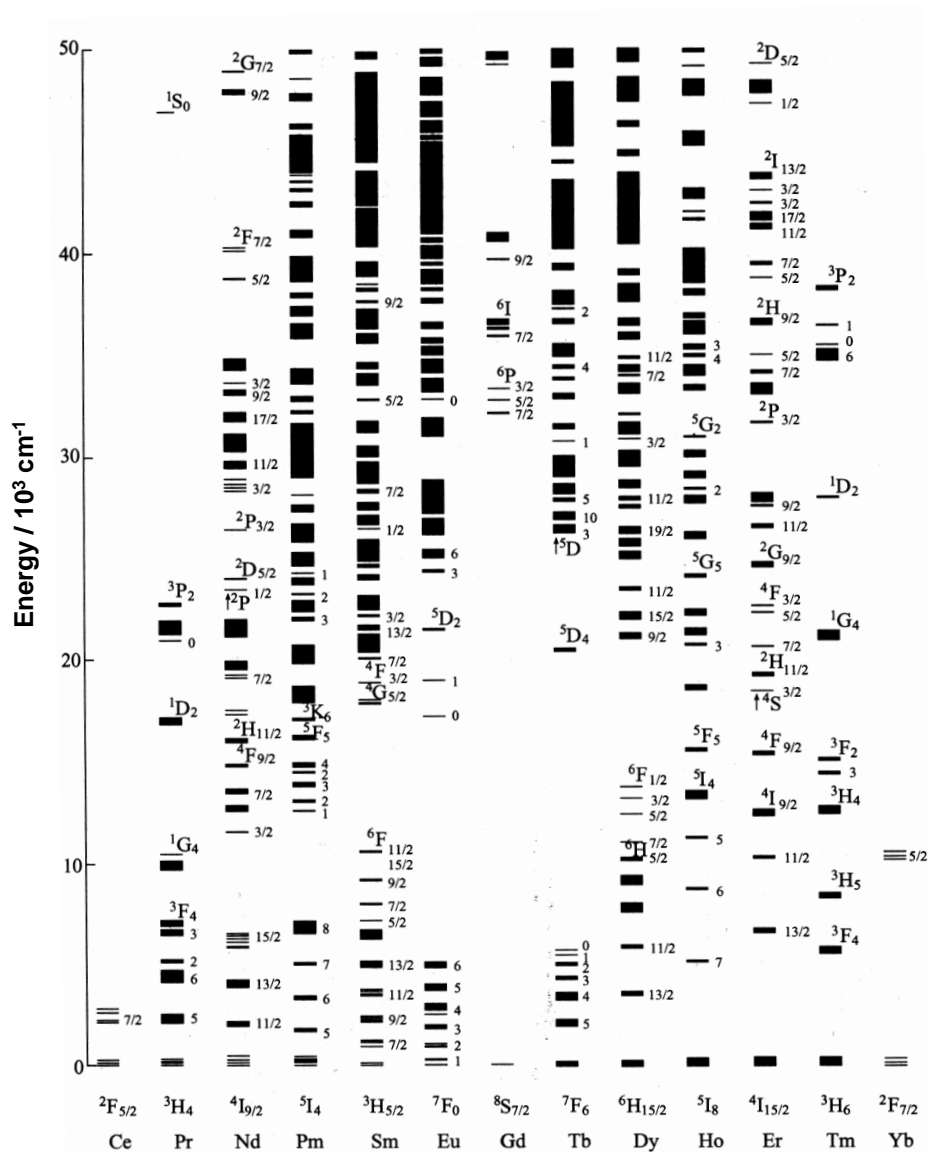


Figure 1. Partial energy level diagram for Ln^{III} ions doped in a low-symmetry crystal, LaF₃. Redrawn from ref.³.

The ligand-field splitting of the $(2J+1)$ degenerate electronic levels, as revealed by absorption or emission spectra, is a useful tool for the determination of the symmetry point group to which the compound belongs. Ligand-field sublevels are identified by their corresponding irreducible representation as deduced from group-theoretical consideration. For instance the $\text{Eu}(^7\text{F}_1)$ level splits in C_3 symmetry into $^7\text{F}_1(\text{A})$ and $^7\text{F}_1(\text{E})$ sublevels, the latter being doubly degenerate.

2. Forbidden Intraconfigurational f-f Transitions

Absorption or emission of photons is promoted by operators linked to the nature of light: the odd-parity electric dipole (ED) operator, the even-parity magnetic dipole (MD) operator and higher order operators such as the electric quadrupole (EQ) operator. Laporte's parity selection rule implies that ED 4f-4f transitions are forbidden. However, when the lanthanoid ion undergoes the influence of a ligand-field, non-centrosymmetric interactions mix electronic states of opposite parity into 4f wavefunctions, which somewhat relaxes the selection rule and the transitions become partially allowed. These transitions are then called *induced* (or forced) electric dipole transition. Contributions to their intensity arise from several sources but major ones are mixing of the $4f^n$ configuration with opposite parity $4f^{n-1}5d^1$ configuration,⁹ ligand-to-metal charge transfer (LMCT) states, and/or vibrational levels. Some induced ED transitions are highly sensitive to small changes in the chemical environment of the metal ion and are denoted *hypersensitive* or sometimes *pseudo-quadrupolar transitions* because they apparently follow the selection rules of EQ transitions. While the intensity of regular ED transitions varies by factors 2-5 depending on the composition of the inner coordination sphere of the metal ion, hypersensitive transitions can be enhanced up to 200-fold.

Table 2. Number of ligand-field sublevels versus site symmetry and the value of the J quantum number.¹

Symmetry	Site symmetry	integer J									
		0	1	2	3	4	5	6	7	8	
Cubic	T, T_d, T_h, O, O_h	1	1	2	3	4	4	6	6	7	
Hexagonal	$C_{3h}, D_{3h}, C_6, C_{6h}, C_{6v}, D_6, D_{6h}$	1	2	3	5	6	7	9	10	11	
Trigonal	$C_3, S_6, C_{3v}, D_3, D_{3d}$										
Tetragonal	$C_4, S_4, C_{4h}, C_{4v}, D_4, D_{2d}, D_{4h}$	1	2	4	5	7	8	10	11	13	
Low	$C_1, C_s, C_2, C_{2h}, C_{2v}, D_2, D_{2h}$	1	3	5	7	9	11	13	15	17	
Symmetry	Site symmetry	half-integer J									
		1/2	3/2	5/2	7/2	9/2	11/2	13/2	15/2	17/2	
Cubic	T, T_d, T_h, O, O_h	1	1	2	3	3	4	5	6	6	
All others ^a	see above	1	2	3	4	5	6	7	8	9	

^a All sublevels are doubly degenerate (Kramer's doublets)

3. *Forbidden Intraconfigurational f-f Transitions*

Absorption or emission of photons is promoted by operators linked to the nature of light: the odd-parity electric dipole (ED) operator, the even-parity magnetic dipole (MD) operator and higher order operators such as the electric quadrupole (EQ) operator. Laporte's parity selection rule implies that ED 4f-4f transitions are forbidden. However, when the lanthanoid ion undergoes the influence of a ligand-field, non-centrosymmetric interactions mix electronic states of opposite parity into 4f wavefunctions, which somewhat relaxes the selection rule and the transitions become partially allowed. These transitions are then called *induced* (or forced) electric dipole transition. Contributions to their intensity arise from several sources but major ones are mixing of the 4fⁿ configuration with opposite parity 4fⁿ⁻¹5d¹ configuration,⁹ ligand-to-metal charge transfer (LMCT) states, and/or vibrational levels. Some induced ED transitions are highly sensitive to small changes in the chemical environment of the metal ion and are denoted *hypersensitive* or sometimes *pseudo-quadrupolar transitions* because they apparently follow the selection rules of EQ transitions. While the intensity of regular ED transitions varies by factors 2-5 depending on the composition of the inner coordination sphere of the metal ion, hypersensitive transitions can be enhanced up to 200-fold.

Magnetic dipole transitions are parity allowed but their intensity is much smaller while the very weak electric-quadrupole transitions have rarely been identified.

In addition to the parity selection rule, other rules are operative, on ΔS , ΔL , ΔJ (see Table 3), as well as symmetry-related selection rules that can be derived from group-theoretical considerations. The 4f-4f transitions are sharp because the electronic rearrangement consecutive to the promotion of an electron into a 4f orbital of higher energy does not perturb much the binding pattern in the molecules (the covalency of Ln^{III}-ligand bonds is at most 5–7 %).

Table 3. Selection rules for intra-configurational f-f transitions

Operator	Parity	ΔS	ΔL	ΔJ^a
ED	opposite	0	≤ 6	≤ 6 (2, 4, 6 if J or $J'=0$)
MD	same	0	0	0, ± 1
EQ	same	0	0, ± 1 , ± 2	0, ± 1 , ± 2

^a $J=0$ to $J'=0$ transitions are always forbidden

Absorption spectra

Intensity of induced ED absorptions are described by Judd-Ofelt (JO) theory⁴ which takes into consideration the 4fⁿ configuration only and which treats spin-orbit coupling within the intermediate coupling scheme. It is noteworthy that molar absorption coefficients are, with a few exceptions, smaller

than $10 \text{ M}^{-1}\text{cm}^{-1}$ and very often smaller than 1 or even $0.1 \text{ M}^{-1}\text{cm}^{-1}$. For an isotropic solid or a solution, the dipole strength of an induced ED f-f absorption between states Ψ and Ψ' , expressed in $\text{esu}^2\text{cm}^2 (=10^{36} \text{ debye}^2)$, is written as:

$$D_{ED} = e^2 \cdot \sum_{\lambda=2,4,6} \Omega_{\lambda} \cdot \left| \langle \Psi \| U^{\lambda} \| \Psi' \rangle \right|^2 \quad (1)$$

in which e is the electric charge of the electron, U^{λ} are the irreducible tensor forms of the ED operator, and Ω_{λ} are the phenomenological Judd-Ofelt parameters, given in cm^2 . The bracketed expressions in eq. (1) are dimensionless doubly-reduced matrix elements which are insensitive to the metal-ion environment and which are tabulated. Mathematical treatment of the parity mixing by the ligand-field perturbation results in the selection rules given in Table 3. Judd-Ofelt parameters are calculated from the absorption spectrum $\varepsilon(\tilde{\nu})$ where $\tilde{\nu}$ is the wavenumber (cm^{-1}). The experimental dipole strength for an isotropic crystal or a solution is defined as:

$$D(\text{exp}) = \frac{10^{36}}{108.9 \cdot \tilde{\nu}_{\text{mean}} \cdot X_A} \cdot \left((2J+1) \cdot \frac{9n}{(n^2+2)^2} \right) \cdot \int \varepsilon(\tilde{\nu}) d\tilde{\nu} \quad (2)$$

with X_A being the fractional population of the initial state while $\tilde{\nu}_{\text{mean}}$ is given by:

$$\tilde{\nu}_{\text{mean}} = \frac{\int \tilde{\nu} \cdot \varepsilon(\tilde{\nu}) d\tilde{\nu}}{\int \varepsilon(\tilde{\nu}) d\tilde{\nu}} \quad (3)$$

The above equations assume that the absorption bands are symmetrical with either Gaussian or Lorentzian bandshape. If not, the following equation has to be substituted for eq. (2):

$$D(\text{exp}) = \frac{10^{36}}{108.9 \cdot X_A} \cdot \left((2J+1) \cdot \frac{9n}{(n^2+2)^2} \right) \cdot \int \frac{\varepsilon(\tilde{\nu})}{\tilde{\nu}} d\tilde{\nu} \quad (4)$$

$(2J+1)$ is the degeneracy of the initial state and the expression involving the refractive index n is known as Lorentz's local-field correction. The theory does not apply equally well to all Ln^{III} ions because calculations of transition probabilities are made assuming that all ligand-field sublevels of the ground level are equally populated, which is not true since there is a Boltzmann distribution of the population among the ligand-field sublevels. Moreover when a 4f-5d state (e.g. in the case of Tb^{III}) or a LMCT state lies relatively close to the excited state implied in the transition, mixing with the 4f wavefunction distorts the results.

In the case of Eu^{III} , calculation of the JO parameters is quite simple since Ω_2 , Ω_4 , and Ω_6 can be directly extracted from the dipole strength of the ${}^5\text{D}_2 \leftarrow {}^7\text{F}_0$, ${}^5\text{D}_4 \leftarrow {}^7\text{F}_0$, and ${}^5\text{L}_6 \leftarrow {}^7\text{F}_0$ transitions, respectively. An example of f-f absorption spectrum and its JO treatment is given in Figure 2 while tabulations of JO parameters can be found in reference² and spectra for all Ln^{III} ions are presented in references^{7,10}

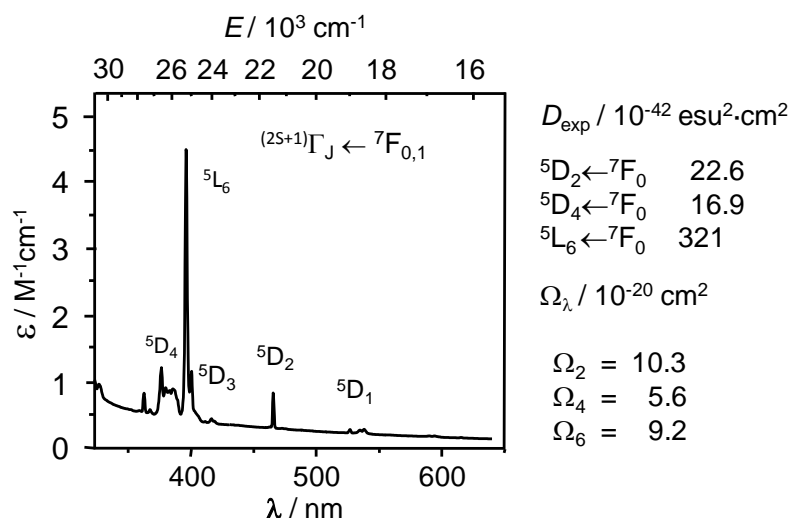


Figure 2. Absorption spectrum of $\text{Cs}_3[\text{Eu}(\text{dpa})_3]$ 1.8×10^{-2} M (dpa is 2,6-pyridine dicarboxylate) in Tris-HCl 0.1 M and associated dipole strengths and JO parameters. Redrawn after ref. ¹¹.

Emission spectra

Except La^{III} and Lu^{III} , all Ln^{III} ions are luminescent and their f-f emission lines cover the entire spectrum, from UV (Gd^{III}) to visible (e.g. Pr^{III} , Sm^{III} , Eu^{III} , Tb^{III} , Dy^{III} , Tm^{III}) and near-infrared (e.g. Pr^{III} , Nd^{III} , Ho^{III} , Er^{III} , Yb^{III}) spectral ranges. Several ions are simultaneous visible and NIR emitters (e.g. Sm^{III} , Eu^{III} , Er^{III} , Tm^{III}). Some ions are fluorescent ($\Delta S = 0$), others are phosphorescent ($\Delta S \neq 0$), and some are both. When the ions are excited directly into f-f transitions, the Stokes' shifts are very small but a different situation prevails in organic molecules for which excitation leads frequently to a lengthening of the chemical bonds, resulting in large Stokes' shifts and since the coupling with vibrations is strong, in broad emission bands. Therefore when Ln^{III} ions are excited by energy transfer from the ligand(s), a process known as sensitization (or antenna effect), the resulting luminescence spectra show large Stokes' shift and narrow, easily recognizable emission bands. This, coupled with the long lifetimes of the 4f excited states (usually micro- to milli-second range) makes Ln^{III} ions ideal probes for all kind of structural and analytical applications. The selection rules listed in Table 3 hold for emission spectra as well.

Important parameters characterizing the emission of light are the lifetime of the excited state $\tau_{\text{obs}} = 1/k_{\text{obs}}$ and the quantum yield Q . The "intrinsic" quantum yield (sometimes referred to as *quantum efficiency*) is related to the rate at which the excited level is depopulated, k_{obs} , and to the radiative rate constant, k_{rad} :

$$Q_{\text{Ln}}^{\text{Ln}} = \frac{k_{\text{rad}}}{k_{\text{obs}}} = \frac{\tau_{\text{obs}}}{\tau_{\text{rad}}} \quad (5)$$

The rate constant k_{obs} is the sum of the rates of the different deactivation processes:

$$k_{obs} = k_{rad} + \sum_n k_n^{nr} = k_{rad} + \sum_i k_i^{vibr}(T) + \sum_j k_j^{pet}(T) + \sum_k k_k^{nr} \quad (6)$$

where k_{rad} and k^{nr} are the radiative and nonradiative rate constants, respectively; the superscript *vibr* points to vibration-induced processes while *pet* refers to photo-induced electron transfer processes such as those generated by LMCT states for instance; the rate constants k' are associated with the remaining deactivation paths. The intrinsic quantum yield depends primarily on the energy gap ΔE between the emissive state of the metal ion and the highest sublevel of its ground, or receiving, multiplet. The smaller this gap, the easier is its bridging by nonradiative deactivation processes, for instance by transfer to the overtones of high-frequency vibrations of bound ligands, particularly O–H, N–H, or C–H (in the case of near-infrared-emitting ions).

Since f-f transitions are very weak, and often obscured by intense ligand absorptions, Q_{Ln}^{Ln} is difficult to measure so that it is commonly estimated from the lifetimes. This requires determination of τ_{rad} which is related to Einstein's rates of spontaneous emission A from an initial state $|\Psi_J\rangle$, characterized by a quantum number J , to a final state $|\Psi'_{J'}\rangle$:

$$A_{rad}(\Psi_J, \Psi'_{J'}) = k_{rad} = \frac{1}{\tau_{rad}} = \frac{64\pi^4 \tilde{\nu}^3}{3h(2J+1)} \left[\frac{n(n^2+2)^2}{9} D_{ED} + n^3 D_{MD} \right] \quad (7)$$

where $\tilde{\nu}$ is the mean energy of the transition defined in eq. (3), h is Planck's constant, n is the refractive index; D_{ED} is given by eq. (1) and D_{MD} by eq. (8):

$$D_{MD} = \left(\frac{e \cdot h}{4 \cdot \pi \cdot m_e \cdot c} \right)^2 \cdot |\langle \Psi || L+2S || \Psi' \rangle|^2 \quad (8)$$

The bracketed matrix elements are tabulated and the radiative lifetime can therefore be extracted from the spectral intensity with the help of eqs. (1), (7), and (8). Except in few cases, this calculation is not trivial and large errors may occur, particularly if the hypotheses pertaining to Judd-Ofelt theory do not hold. There are however special cases for which determination of τ_{rad} is easier.

The first one is when the absorption spectrum to the emissive level is known, which the case is when luminescence transitions terminate onto the ground level; the radiative lifetime can then be simply calculated from the following equation where N_A is Avogadro's number (6.023×10^{23}):

$$\frac{1}{\tau_{rad}} = 2303 \times \frac{8\pi c n^2 \tilde{\nu}^2 (2J+1)}{N_A (2J'+1)} \int \varepsilon(\tilde{\nu}) d\tilde{\nu} \quad (9)$$

The second case applies to Eu^{III} for which one emission transition has pure magnetic origin (${}^5\text{D}_0 \rightarrow {}^7\text{F}_1$) and is therefore a convenient standard for JO parameterization,^{10,12} so that a simplified equation can be derived:¹³

$$A(\Psi_J, \Psi'_{J'}) = \frac{1}{\tau_{rad}} = A_{MD,0} \cdot n^3 \left(\frac{I_{tot}}{I_{MD}} \right) \quad (10)$$

with $A_{MD,0}$ being equal to 14.65 s^{-1} ; (I_{tot}/I_{MD}) is the total integrated emission from the $\text{Eu}({}^5\text{D}_0)$ level to the ${}^7\text{F}_J$ manifold ($J = 0-6$) divided by the integrated intensity of the ${}^5\text{D}_0 \rightarrow {}^7\text{F}_1$ MD transition.

When excitation occurs through absorption into the ligand levels followed by energy transfer onto one of the Ln^{III} excited state, the corresponding quantum yield is called “overall” quantum yield:

$$Q_{Ln}^L = \eta_{sens} \cdot Q_{Ln}^{Ln} = \eta_{sens} \cdot \frac{\tau_{obs}}{\tau_{rad}} \quad (11)$$

Quantification of the sensitization efficiency (η_{sens}) can be made if both the intrinsic and overall quantum yields are known. Figure 3 describes the sensitization process in a very simplified way. The donor state can be a singlet state, a triplet state (a common situation), a charge transfer state, a 4f5d state, or a d-transition metal state. A detailed discussion is presented in reference¹⁴ particularly with respect to the role of triplet and charge transfer states and to the detrimental effect of vibrations; NIR-emitting ions are especially sensitive to nonradiative vibrational deactivations.¹⁵

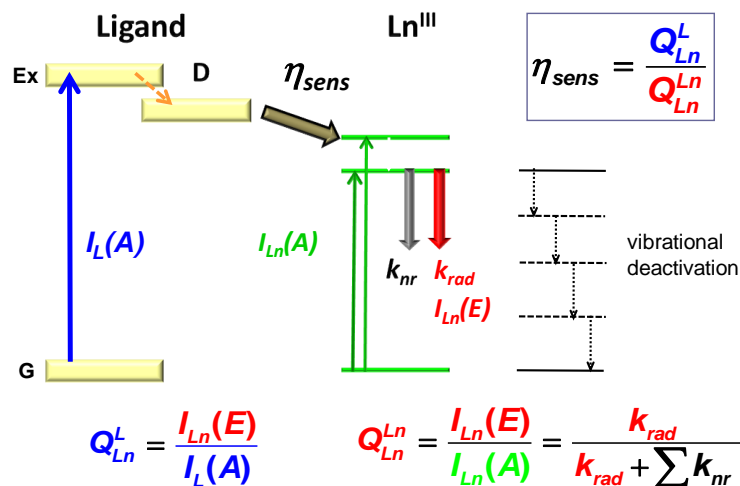


Figure 3. Simplified scheme demonstrating sensitization of Ln^{III} luminescence by a ligand. Key: A = absorption, E = emission, G = ground state, Ex = excited state, D = donor state; other parameters are defined in text.

3 Allowed 5d-4f and Charge Transfer Transitions

Interconfigurational $4f^n \leftrightarrow 4f^{n-1}5d^1$ transitions are parity allowed.¹⁶ They feature broader bands than f-f transitions and their energy is highly dependent on the ligand-field strength since 5d orbitals have large radial

expansion, allowing extensive tuning of the absorption and/or emission wavelengths. However, these transitions are highly energetic (Figure 4) so that they are usually observed for Ce^{III}, Pr^{III}, and Tb^{III} only.

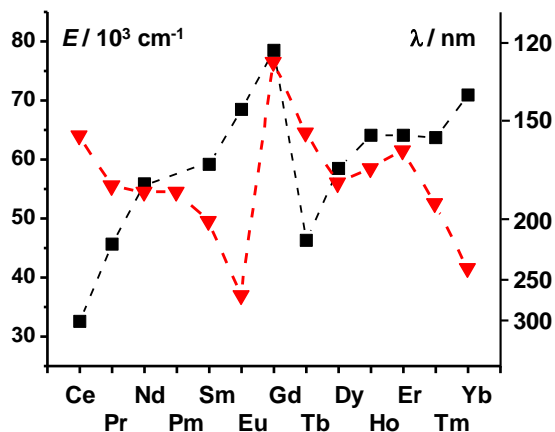


Figure 4. Energies and corresponding wavelengths of the 4f-5d transitions in CaF₂:Ln^{III} (squares) and 2p(O)-4f LMCT transitions (triangles). Redrawn from ref.⁶.

Similarly, charge-transfer transitions, either LMCT or MLCT (metal-to-ligand charge transfer) are also allowed and usually occur at high energies since they correspond to either reduction or oxidation of the metal ion. Typically, the lowest energies for LMCT transitions are associated with easily reducible ions such as Sm^{III}, Eu^{III}, Tm^{III}, or Yb^{III} (Figure 4). In organic complexes, mixing with ligand orbitals can lower the LMCT energy down to 18-20 000 cm⁻¹ for Eu^{III}.¹⁴ LMCT states behave differently with respect to luminescence properties depending on their energy. For Eu^{III}, severe quenching occurs for $E_{LMCT} < 22\text{-}25\ 000 \text{ cm}^{-1}$, while these states can be used as luminescence sensitizer when they lie above 25 000 cm⁻¹. MLCT states which are common in d-transition metal complexes are rarely identified in spectra of lanthanoid compounds, except for Ce^{III}, the oxidation of which into Ce^{IV} is facile, and, possibly, Tb^{III}.

References

- 1 C. Görller-Walrand and K. Binnemans, in *Handbook on the Physics and Chemistry of Rare Earths*, eds. Gschneidner Jr., K. A. and Eyring, L., Vol. 23, Ch.155, Elsevier Science B.V., Amsterdam, 1996.
- 2 C. Görller-Walrand and K. Binnemans, in *Handbook on the Physics and Chemistry of Rare Earths*, eds. Gschneidner Jr., K. A. and Eyring, L., Vol. 25, Ch.167, Elsevier Science B.V., Amsterdam, 1998.
- 3 *Spectroscopic Properties of Rare Earths in Optical Materials*, Tsinghua University Press & Springer Verlag, Beijing & Heidelberg, 2005.
- 4 B. M. Walsh, in *Advances in Spectroscopy for Lasers and Sensing*, ed. B. Di Bartolo and O. Forte, Springer Verlag, Berlin, 2006, 403-33.

- 5 P. Hänninen and H. Härmä, in *Springer Series on Fluorescence*, eds. Wolfbeis, O. S. and Hof, M., Vol. 7., Springer Verlag, Berlin, 2011.
- 6 J.-C. G. Bünzli and S. V. Eliseeva, in *Springer Series on Fluorescence. Lanthanide Luminescence: Photophysical, Analytical and Biological Aspects*, eds. Wolfbeis, O. S. and Hof, M., Vol. 7, Springer Verlag, Berlin, 2011.
- 7 W. T. Carnall, in *Handbook on the Physics and Chemistry of Rare Earths*, eds. Gschneidner Jr., K. A. and Eyring, L., Vol. 3, Ch.24, North Holland Publ. Co., Amsterdam, 1979.
- 8 S. Hüfner, *Optical Spectra of Transparent Rare Earth Compounds*, Academic Press, New York, 1978.
- 9 G. K. Liu, in *Spectroscopic Properties of Rare Earths in Optical Materials*, ed. G. K. Liu and B. Jacquier, Springer Verlag, Berlin, 2005, Vol.83, Ch. 1, 1-94.
- 10 C. Görller-Walrand and L. Fluyt, in *Handbook on the Physics and Chemistry of Rare Earths*, eds. Gschneidner Jr., K. A., Bünzli, J.-C. G., and Pecharsky, V. K., Vol. 40, Ch. 244, Elsevier Science B.V., Amsterdam, 2010.
- 11 A. Aebischer, F. Gumy and J.-C. G. Bünzli, *Phys. Chem. Chem. Phys.*, 2009, **11**, 1346.
- 12 C. Görller-Walrand, L. Fluyt, A. Ceulemans and W. T. Carnall, *J. Chem. Phys.*, 1991, **95**, 3099.
- 13 M. H. V. Werts, R. T. F. Jukes and J. W. Verhoeven, *Phys. Chem. Chem. Phys.*, 2002, **4**, 1542.
- 14 J.-C. G. Bünzli and S. V. Eliseeva, in *Comprehensive Inorganic Chemistry II*, ed. V. W.-W. Yam, Elsevier B.V., Amsterdam, 2013, Vol.8, Ch. 8.03, in press.
- 15 S. Comby and J.-C. G. Bünzli, in *Handbook on the Physics and Chemistry of Rare Earths*, eds. Gschneidner Jr., K. A., Bünzli, J.-C. G., and Pecharsky, V. K., Vol. 37, Ch. 235, Elsevier Science B.V., Amsterdam, 2007.
- 16 G. W. Burdick and M. F. Reid, in *Handbook on the Physics and Chemistry of Rare Earths*, eds. Gschneidner Jr., K. A., Bünzli, J.-C. G., and Pecharsky, V. K., Vol. 37, Ch. 232, Elsevier Science B.V., Amsterdam, 2007.